

SUPPORTING INFORMATION

Inorganic Salts in Purely Ionic Liquid Media: The Development of High Ionicity Ionic Liquids (HIILs)

Ana B. Pereiro,^{a*} João M. M. Araújo,^a Filipe S. Oliveira,^a Carlos E. S. Bernardes,^b José M. S. S. Esperança,^a José N. Canongia Lopes,^{a,b} Isabel M. Marrucho^a and Luís P. N. Rebelo^{a,*}

^aInstituto de Tecnologia Química e Biológica, www.itqb.unl.pt, UNL, Av. da República, 2780-157 Oeiras, Portugal

^bCentro de Química Estrutural, IST/UTL, 1049-001 Lisboa, Portugal

*Corresponding Author: anab@itqb.unl.pt (Ana B. Pereiro) and luis.rebelo@itqb.unl.pt (Luís P. N. Rebelo)

Experimental Section

Materials

All ionic liquids (ILs) and inorganic salts (ISs) used in this study are described in Table S1, including their source and purity. Ionic liquids prepared at QUILL were characterized by a combination of ¹H NMR, ¹³C NMR, electrospray ionisation mass spectrometry, halide content determination, CHN elemental analysis, and water content assay techniques. Typical halide content was $\leq 0.1\%$.

To reduce the water and other volatile substances contents, vacuum (3×10^{-2} Torr) and moderate temperature (ca. 318.15 K) were always applied to all samples of both ionic liquid and inorganic salt for several days prior to their use. The final water mass fraction was measured by Karl Fischer coulometric titration (Metrohm 831 KF Coulometer). The dried ionic liquids contained less than 1200 ppm of water. The purity of all ionic liquids was checked by ¹H NMR.

Initial Screening and Solubility measurements

Screening of the solubility of inorganic salts in a wide variety of ILs was accomplished using a visual detection method. The solubility limit was detected by the appearance of a precipitate as a consequence of repeated addition of 1–2 mg of inorganic salt to approximately 1 g of IL, with continuous stirring, at room temperature and atmospheric pressure.

The precise quantitative determination of the solubility of [NH₄][SCN] in [C₂MIM][C₂SO₄] and in [C₂MIM][OAc] was performed using a Thermomixer Comfort (Eppendorf). The solubility measurements were carried out at 298.15 K, whilst stirring at up to 1400 r · min⁻¹. Approximately 0.250 g of ionic liquid was placed inside the safe-lock micro test tubes and an excess amount of the inorganic salt was added at a constant temperature. The uncertainty in this variable is ± 0.1 K. Since the safe-lock micro test tubes are conical at the bottom, it was important to add the solid at the end of the process to guarantee that the equilibrium occurred efficiently. A study of the solubility with time was carried out with aim to ensure that the equilibrium was achieved. Before sampling, each solution was centrifuged (30 min) to enhance the physical separation of the liquid and solid phases. Triplicates of each sample were always measured.

Attenuated Total Reflection Fourier Transform Infra Red (ATR-FTIR) Spectroscopy was implemented to quantitatively evaluate the amount of ammonium thiocyanate solubilized in [C₂MIM][C₂SO₄] and in [C₂MIM][OAc]. This procedure allows the accurate assay of the solubility of the inorganic salt in the ionic liquid. The infrared spectra of the neat IL / IS and the [NH₄][SCN] / [C₂MIM][C₂SO₄] or [C₂MIM][OAc] solutions were recorded by means of an IFS-66/S FTIR spectrometer from Bruker (Bruker Daltonics, MA, USA) using a single reflection ATR cell (DuraDisk). Acquisition was accomplished in the DTGS-detection mode using an accumulation rate of 258 scans at a resolution of 8 cm⁻¹ at room temperature in the spectral range of 4000–600 cm⁻¹ and was processed using the Opus software package (Bruker) with a wavenumber accuracy of 0.1 cm⁻¹. Any interference due to water vapor and CO₂ was avoided by purging the sample and detector compartments with N₂, at a flow rate of 18 L min⁻¹.

Acetic Acid Content in the [C₂MIM][OAc] + [NH₄][SCN] Mixture

Different samples of [C₂MIM][OAc] + [NH₄][SCN] binary mixture at x [NH₄][SCN] ≈ 0.33 (composition close to the solubility limit) were prepared gravimetrically using an analytical high-precision balance with an uncertainty of $\pm 10^{-5}$ g. The acetic acid [HOAc] content present in the binary mixture was studied as a function of time to obtain the maximum acetic acid content at different temperatures (298.15 K and 333.15 K). ATR-FTIR spectra of all samples were analyzed with the time to calculate acetic acid content in the sample. Triplicates of each sample were always measured. The uncertainty of the composition resulted in an estimation of ± 0.0003 in mass fraction.

Viscosity and density measurements

Viscosity and density were measured in the temperature range between 298.15 and 333.15 K at atmospheric pressure using an automated SVM 3000 Anton Paar rotational Stabinger viscometer-densimeter. The SVM 3000 uses Peltier elements for fast and efficient thermostability. The temperature uncertainty is ± 0.02 K. The precision of the dynamic viscosity measurements is $\pm 0.5\%$ and the absolute uncertainty of the density is ± 0.0005 g·cm⁻³. The overall uncertainty of the viscosity measurements (taking into account the purity and handling of the samples) is estimated to be 2 %.^{S3} Further details

about the equipment and method can be found elsewhere.^{S4} For each sample, triplicates were measured and the reported result is the average value.

Table S1. Description of the ionic liquids and inorganic salts used in the solubility screening of inorganic salts in a wide range of ionic liquids.

Formal Name	Structure	Abbreviation	Supplier and Purity %
Ionic Liquids			
1-Ethyl-3-methylimidazolium Acetate		[C ₂ MIM][OAc]	Iolitec 95%
1-Ethyl-3-methylimidazolium Thiocyanate		[C ₂ MIM][SCN]	Iolitec 98%
1-Ethyl-3-methylimidazolium Ethylsulfonate		[C ₂ MIM][C ₂ SO ₃]	Prepared according to Ref.S1
1-Ethyl-3-methylimidazolium Ethylsulfate		[C ₂ MIM][C ₂ SO ₄]	Iolitec 99%
1-Ethyl-3-methylimidazolium Bis(trifluoromethylsulfonyl)imide		[C ₂ MIM][NTf ₂]	Iolitec 99%
1-Ethyl-3-methylimidazolium Trifluoromethanesulfonate		[C ₂ MIM][OTf]	Iolitec 99%
1-Ethyl-3-methylimidazolium Tetracyano-borate		[C ₂ MIM][B(CN) ₄]	Solvent Innovation 98%
1-Ethyl-3-methylimidazolium Tris(pentafluoroethyl)trifluorophosphate		[C ₂ MIM][PF ₃ (C ₂ F ₅) ₃]	Solvent Innovation 98%
Trihexyl(tetradecyl)phosphonium Bis(trifluoromethylsulfonyl)imide		[P ₆₆₆₁₄][NTf ₂]	Iolitec 99%
Trihexyl(tetradecyl)phosphonium L-Lactate		[P ₆₆₆₁₄][L-Lactate]	Prepared by QUILL
Trihexyl(tetradecyl)phosphonium Trifluoromethanesulfonate		[P ₆₆₆₁₄][OTf]	Iolitec 98%
Butylmethylphosphonium Methylsulfate		[P ₄₄₄₁][C ₁ SO ₄]	Cytec 99%
2-Hydroxyethyl(trimethyl)ammonium L-Lactate		[Ch][L-Lactate]	Prepared by QUILL
Ethyl(2-hydroxyethyl)dimethylammonium Bis(trifluoromethylsulfonyl)imide		[EtCh][NTf ₂]	Prepared according to Ref.S2
Inorganic Salts			
Sodium Thiocyanate	$\text{Na}^+ \text{S}=\text{C}=\text{N}^-$	[Na][SCN]	Fluka 98%
Sodium Cyanate	$\text{Na}^+ \text{O}=\text{C}=\text{N}^-$	[Na][OCN]	Sigma – Aldrich 96%
Sodium Chloride	$\text{Na}^+ \text{Cl}^-$	[Na][Cl]	Sigma – Aldrich 99.5%

Sodium Sulfate		[Na ₂][SO ₄]	Fluka 99%
Calcium Chloride		[Ca][Cl ₂]	Sigma – Aldrich 97%
Ammonium Chloride		[NH ₄][Cl]	Sigma – Aldrich 99.5%
Ammonium Thiocyanate		[NH ₄][SCN]	Sigma – Aldrich 97.5%

Ionic conductivity measurements

Ionic conductivities were performed using a CDM210 Radiometer Analytical conductivimeter. Measurements were performed in a glass cell containing a magnetic stirrer and temperature regulated by a water jacket connected to a bath controlled to $\pm 0.01\text{K}$. The temperature in the cell was measured by means of a platinum resistance thermometer coupled to a Keithley 199 System DMM/Scanner. The thermometer was calibrated with high-accuracy mercury thermometers (0.01 K). For the ionic conductivity measurements, 1.5 ml of the sample was added to the thermostatic cell and vigorously stirred. The cell was closed with screw caps to ensure a secure seal and flushed with dry nitrogen to prevent humidity. Each single measurement was performed as quickly as possible to minimize undesired effects (such as self-heating of the samples, ionization in the electrodes, etc)^{55,56} that might modify the measured conductivity values. This conductivimeter uses an alternating current of 12 V and $2.93\text{--}23.4\text{ kHz}$ of frequency in the range of conductivities measured in this work. The use of high frequency alternating current (greater than 600Hz) and the fact that the electrodes were platinised avoided the polarization phenomena that can occur at the surface of the cell electrodes.^{55,57} The conductivimeter had been previously calibrated at each temperature with certified 0.01D and 0.1 D KCl standard solutions supplied by Radiometer Analytical. This technique was validated using the pure ionic liquids 1-ethyl-3-methylimidazolium bis(trifluoromethylsulfonyl)imide ($[\text{C}_2\text{MIM}][\text{NTf}_2]$) and 1-hexyl-3-methylimidazolium bis(trifluoromethylsulfonyl)imide ($[\text{C}_6\text{MIM}][\text{NTf}_2]$). The obtained results were compared with the published data using the impedance method,^{58,59} showing maximum relative deviations of 2 % . Every conductivity value was determined at least three times to ensure its reproducibility within 1 % in absolute value.

NMR studies

To analyze the changes in the ^1H and ^{13}C chemical shifts of the ionic liquid with increasing $[\text{NH}_4][\text{SCN}]$ concentration, samples were prepared gravimetrically using an analytical high-precision balance with an uncertainty of $\pm 10^{-5}\text{ g}$, by adding different amounts of $[\text{NH}_4][\text{SCN}]$ into solutions of 0.5 g ionic liquid and 0.5 g deuterated dimethyl sulfoxide (DMSO-d₆). Upon complete dissolution, the samples were transferred to 5 mm NMR tubes containing the same amount of DMSO-d₆. Similarly, to analyze the effect in the ^1H and ^{13}C chemical shifts of $[\text{NH}_4][\text{SCN}]$ with increasing ionic liquid concentration, samples were prepared by adding different quantities of ionic liquid into solutions of 0.4 g $[\text{NH}_4][\text{SCN}]$ and 1.47 g DMSO-d₆. All spectra were obtained using DMSO-d₆, for field-frequency lock and NMR internal reference. As reported in previous studies,⁵⁰ the addition of DMSO-d₆ as a co-solvent has no impact on the chemical shifts trends obtained upon IS or IL addition. All experiments were carried out on a Bruker AVANCE 400 spectrometer operated at room temperature with 16 scans for ^1H NMR and 500 scans for ^{13}C NMR.

Results and Discussion

Initial Screening

Screening of the solubility of inorganic salts in a wide variety of ILs was performed in order to establish the most promising ionic liquids that can be used as solvents. Figure S1 shows the matrix of the systems ionic liquid + inorganic salt studied for mapping the general behaviour present in these binary mixtures. The binary mixtures which contained the inorganic salt ammonium thiocyanate were those that yielded higher solubility limits. Binary mixtures $[\text{C}_2\text{MIM}][\text{C}_2\text{SO}_4]$ or $[\text{C}_2\text{MIM}][\text{OAc}]$ + $[\text{NH}_4][\text{SCN}]$ have been chosen from initial solubility screening as example of the best binary mixtures.

Solubility

The accurate solubility at 298.15 K of ammonium thiocyanate in $[\text{C}_2\text{MIM}][\text{C}_2\text{SO}_4]$ or $[\text{C}_2\text{MIM}][\text{OAc}]$ was determined using ATR-FTIR. The spectra of $[\text{NH}_4][\text{SCN}]$ and $[\text{C}_2\text{MIM}][\text{C}_2\text{SO}_4]$ are depicted in Figure S2a. The vibration modes of the ammonium thiocyanate in the spectra region between 2100 and 2015 cm^{-1} are associated mainly to the C=N bond stretching motions^{51,52} of the $[\text{SCN}]^-$ anion. The ionic liquid does not show any absorbance in this frequency interval. Linear calibration functions were obtained by means of the absolute peak intensity of this characteristic band versus the $[\text{NH}_4][\text{SCN}]$ concentration, as illustrated in Figure S2b.

In order to ensure that equilibrium was achieved, we studied solubility over time. The times frame needed for achieving equilibrium at 298.15K were 30 min for the $[\text{C}_2\text{MIM}][\text{C}_2\text{SO}_4] + [\text{NH}_4][\text{SCN}]$ mixture and 5760 min for the $[\text{C}_2\text{MIM}][\text{OAc}] + [\text{NH}_4][\text{SCN}]$ mixture. The studies were conducted until the difference among consecutive solubility measurements was less than 0.8 % . The molar fraction solubilities of ammonium thiocyanate in the studied ionic liquids at 298.15 K are: 0.6479 for

[C₂MIM][C₂SO₄] and 0.4035 for [C₂MIM][OAc]. It is clear that these ionic liquids are good solvents for the [NH₄][SCN] inorganic salt.

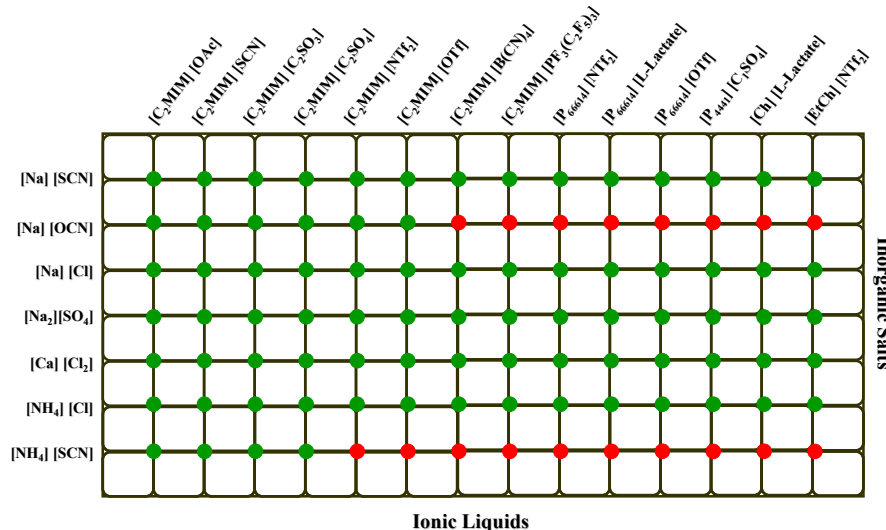


Figure S1. Matrix of the binary mixtures ionic liquids plus inorganic salts studied in this work with aim to map general behaviour. The green dots are the tested binary systems.

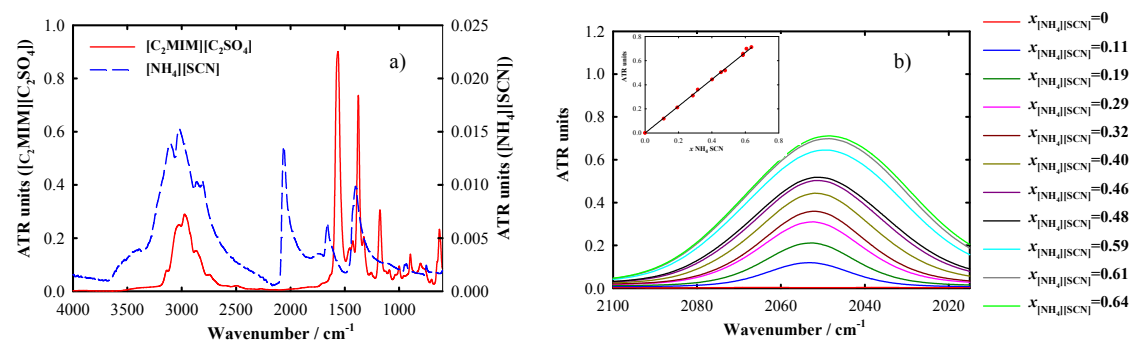
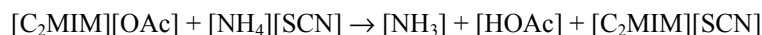


Figure S2. (a) Representative ATR-FTIR spectra of pure ionic liquid [C₂MIM][C₂SO₄] and of pure inorganic salt [NH₄][SCN]; (b) ATR-FTIR spectra of [NH₄][SCN] in [C₂MIM][C₂SO₄] solution in the range of the C=N stretching vibration. Inside figure, calibration of the absolute peak intensity in the range of the C=N stretching vibration as a function of [NH₄][SCN] concentration.

Determination Acetic Acid Content

The binary mixture [C₂MIM][OAc] + [NH₄][SCN] could be considered a protic system where the following reaction could occur:



In order to verify this possible reaction, ATR-FTIR spectroscopy was used to calculate the acetic acid content at 298.15 and 333.15 K. The absorption band between 1747 and 1669 cm⁻¹ in the [HOAc] spectrum is associated mainly to the C=O bond stretching vibration.^{S13} The ionic liquid [C₂MIM][OAc] does not show any absorbance in this frequency interval. Linear calibration functions were obtained at the maximum absorbance value of this characteristic band versus the [HOAc] concentration.

The acetic acid content present in the binary mixture [C₂MIM][OAc] + [NH₄][SCN] was determined versus time to ensure that equilibrium was achieved. As follows from the data in Figure S3, the maximum amount of [HOAc] present in the binary mixtures at 298.15 and 333.15 K is $w[\text{HOAc}] = 0.0199$ and 0.0409 , respectively. These values can be considered negligible, given the evaluated amounts of acetic acid and its constant behaviour with time (almost fifty days time elapsed). Moreover, many pure ionic liquids are sold commercially with a purity of 95 %, as example [C₂MIM][OAc] (IoLiTec GmbH, > 95 %), 1-butyl-3-methylimidazolium acetate (BASF Corporation, ≥ 95 %), 1-ethyl-3-methylimidazolium 1,1,2,2-tetrafluoroethanesulfonate (ALDRICH, ≥ 95 %), tri(n-butyl)ethylphosphonium diethylphosphate (CYTEC, 95 %), trihexyl(tetradecyl)phosphonium decanoate (CYTEC, 94%), and trihexyl(tetradecyl)phosphonium bis 2,4,4-(trimethylpentyl)phosphinate (CYTEC, 93.7 %).

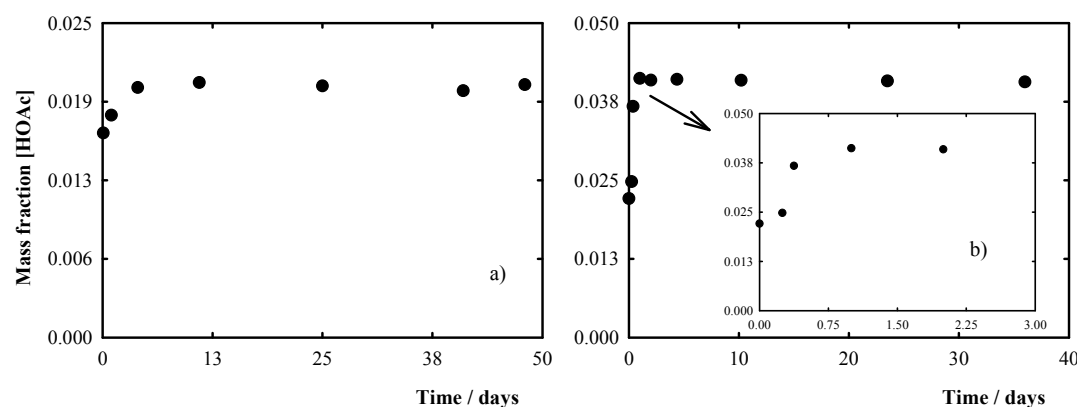


Figure S3 Acetic acid content in $[\text{C}_2\text{MIM}][\text{OAc}] + [\text{NH}_4][\text{SCN}]$ binary mixture versus time in the following conditions: (a) 298.15 K and (b) 333.15 K. Inside figure shows in enlarged scale the Figure S3b.

Density and Viscosity

The measured density and viscosity data for the binary mixtures $[\text{C}_2\text{MIM}][\text{C}_2\text{SO}_4]$ or $[\text{C}_2\text{MIM}][\text{OAc}] + [\text{NH}_4][\text{SCN}]$ as a function of inorganic salt concentration at different temperatures (298.15 K to 333.15 K) are given in Table S2. These data are also shown in Figures S4 and S5 as a function of ammonium thiocyanate concentration. The measured density values for the binary mixture $[\text{C}_2\text{MIM}][\text{C}_2\text{SO}_4] + [\text{NH}_4][\text{SCN}]$ decrease with increasing $[\text{NH}_4][\text{SCN}]$ concentration but these values stabilize at $x[\text{NH}_4][\text{SCN}] \approx 0.5$, close to the solubility limit. In contrast, the density data for the binary mixture $[\text{C}_2\text{MIM}][\text{OAc}] + [\text{NH}_4][\text{SCN}]$ increase with inorganic salt concentration stabilizing at $x[\text{NH}_4][\text{SCN}] \approx 0.2$.

Upon the addition the ammonium thiocyanate salt, viscosity clearly increased from the pure ionic liquid up to $x[\text{NH}_4][\text{SCN}] \approx 0.35$ for $[\text{C}_2\text{MIM}][\text{C}_2\text{SO}_4]$ (where a maximum is observed, as pictured in Figure S5a) and to $x[\text{NH}_4][\text{SCN}] \approx 0.2$ for $[\text{C}_2\text{MIM}][\text{OAc}]$.

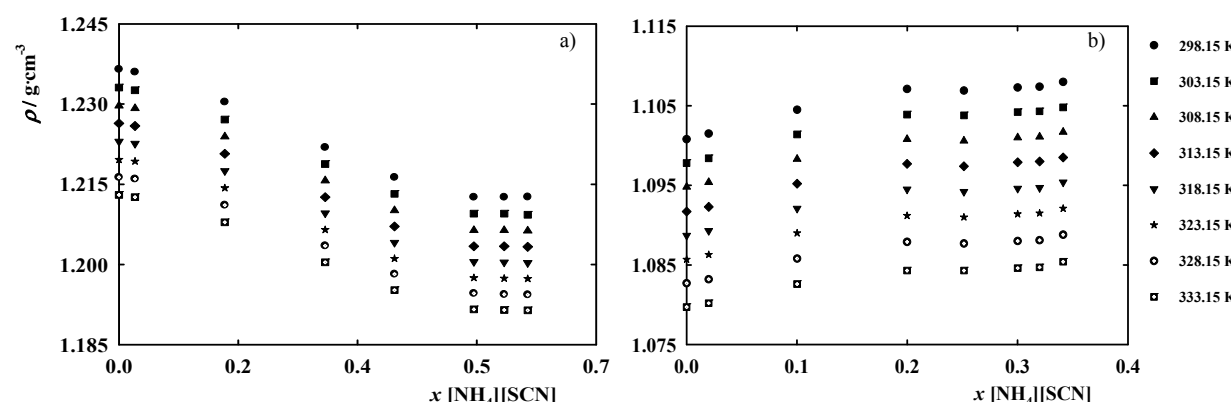


Figure S4. Density as a function of $[\text{NH}_4][\text{SCN}]$ concentration in the solubility range for the binary systems: (a) $[\text{C}_2\text{MIM}][\text{C}_2\text{SO}_4] + [\text{NH}_4][\text{SCN}]$ and (b) $[\text{C}_2\text{MIM}][\text{OAc}] + [\text{NH}_4][\text{SCN}]$.

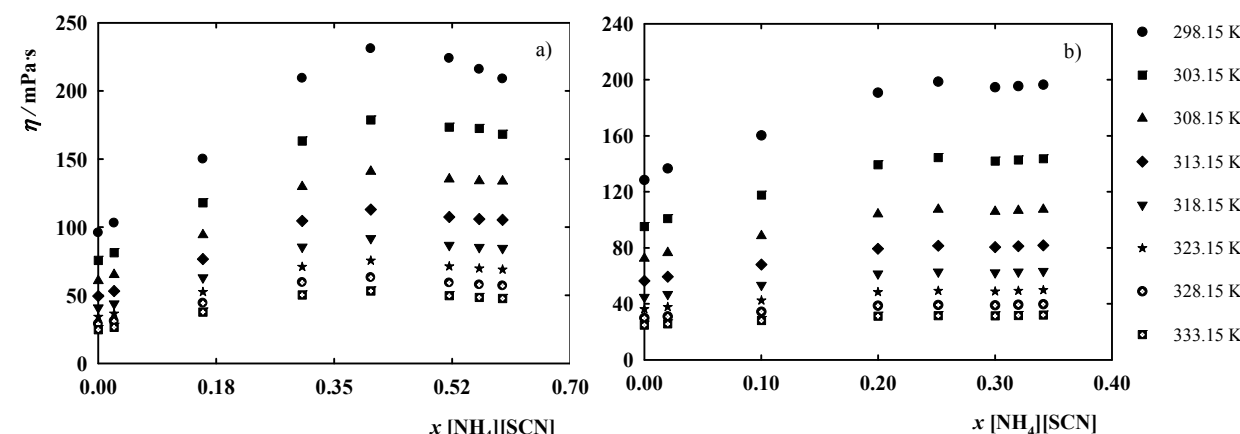


Figure S5. Dynamic viscosity as a function of $[\text{NH}_4][\text{SCN}]$ in the solubility range for the binary systems: (a) $[\text{C}_2\text{MIM}][\text{C}_2\text{SO}_4] + [\text{NH}_4][\text{SCN}]$ and (b) $[\text{C}_2\text{MIM}][\text{OAc}] + [\text{NH}_4][\text{SCN}]$.

Table S2. Density, ρ , dynamic viscosity, η , and ionic conductivity, σ , for the binary systems $[\text{C}_2\text{MIM}][\text{C}_2\text{SO}_4]$ or $[\text{C}_2\text{MIM}][\text{OAc}]$ (1) + $[\text{NH}_4]\text{[SCN]}$ (2) at several temperatures.

x_2	ρ (g·cm ⁻³)	η (mPa·s)	σ (mS·cm ⁻¹)	ρ (g·cm ⁻³)	η (mPa·s)	σ (mS·cm ⁻¹)	ρ (g·cm ⁻³)	η (mPa·s)	σ (mS·cm ⁻¹)	ρ (g·cm ⁻³)	η (mPa·s)	σ (mS·cm ⁻¹)	
[C ₂ MIM][C ₂ SO ₄] + [NH ₄][SCN]													
$T = 298.15 \text{ K}$				$T = 303.15 \text{ K}$				$T = 308.15 \text{ K}$				$T = 313.15 \text{ K}$	
0	1.2365	95.90	3.798	1.2331	75.63	4.676	1.2297	60.66	5.659	1.2264	49.45	6.752	
0.0235	1.2360	103.09	3.732	1.2326	81.26	4.612	1.2292	65.16	5.605	1.2259	53.09	6.704	
0.1553	1.2304	150.02	3.187	1.2271	117.97	3.975	1.2239	94.31	4.859	1.2207	76.57	5.844	
0.3025	1.2219	209.35	2.851	1.2188	163.27	3.576	1.2157	129.64	4.390	1.2126	104.59	5.306	
0.4042	1.2163	231.06	2.793	1.2132	178.67	3.526	1.2101	140.90	4.356	1.2071	112.90	5.263	
0.5205	1.2126	223.95	2.806	1.2095	173.38	3.580	1.2064	135.26	4.459	1.2034	107.48	5.464	
0.5650	1.2126	215.89	2.951	1.2095	172.51	3.754	1.2064	133.91	4.680	1.2034	105.98	5.731	
0.5997	1.2126	208.93	3.012	1.2093	168.24	3.849	1.2063	133.71	4.809	1.2033	105.41	5.897	
$T = 318.15 \text{ K}$				$T = 323.15 \text{ K}$				$T = 328.15 \text{ K}$				$T = 333.15 \text{ K}$	
0	1.2230	40.88	8.555	1.2196	34.24	10.005	1.2163	28.99	—	1.2130	24.81	—	
0.0235	1.2226	43.86	8.455	1.2193	36.68	9.895	1.2160	31.04	—	1.2126	26.54	—	
0.1553	1.2175	63.03	7.385	1.2143	52.56	8.670	1.2111	44.26	—	1.2079	37.68	—	
0.3025	1.2096	85.57	6.335	1.2065	70.90	7.950	1.2035	59.41	—	1.2004	50.29	—	
0.4042	1.2041	91.83	6.327	1.2011	75.56	7.950	1.1982	63.04	—	1.1952	53.18	—	
0.5205	1.2005	86.87	6.565	1.1975	71.22	8.310	1.1946	59.16	—	1.1916	49.72	—	
0.5650	1.2004	85.31	7.280	1.1974	69.75	8.675	1.1944	57.79	—	1.1915	48.47	—	
0.5997	1.2003	84.57	7.510	1.1973	68.92	8.965	1.1943	56.96	—	1.1914	47.67	—	
[C ₂ MIM][OAc] + [NH ₄][SCN]													
$T = 298.15 \text{ K}$				$T = 303.15 \text{ K}$				$T = 308.15 \text{ K}$				$T = 313.15 \text{ K}$	
0	1.1008	128.38	2.950	1.0978	95.11	3.825	1.0948	72.38	4.829	1.0917	56.38	5.995	
0.0200	1.1015	136.61	2.944	1.0984	100.86	3.819	1.0954	76.44	4.832	1.0923	59.28	6.007	
0.1002	1.1045	160.24	2.844	1.1014	117.64	3.712	1.0983	88.53	4.728	1.0952	68.07	5.927	
0.1998	1.1071	190.73	2.961	1.1039	139.29	3.858	1.1008	104.02	4.915	1.0977	79.27	6.171	
0.2514	1.1069	198.58	3.143	1.1038	144.37	4.111	1.1006	107.37	5.248	1.0974	81.46	6.6000	
0.3001	1.1073	194.56	3.439	1.1042	141.95	4.471	1.1010	105.87	5.685	1.0979	80.50	7.820	
0.3199	1.1074	195.42	3.533	1.1043	142.77	4.576	1.1011	106.60	5.802	1.0980	81.14	7.975	
0.3413	1.1080	196.39	3.582	1.1048	143.58	4.633	1.1017	107.30	5.868	1.0985	81.73	8.075	
$T = 318.15 \text{ K}$				$T = 323.15 \text{ K}$				$T = 328.15 \text{ K}$				$T = 333.15 \text{ K}$	
0	1.0887	44.81	8.190	1.0857	36.27	9.840	1.0827	29.81	—	1.0797	24.86	—	
0.0200	1.0893	46.92	8.195	1.0863	37.79	9.855	1.0832	30.91	—	1.0802	25.64	—	
0.1002	1.0921	53.32	8.115	1.0890	42.45	9.865	1.0858	34.29	—	1.0826	28.06	—	
0.1998	1.0945	61.47	8.515	1.0912	48.40	10.390	1.0879	38.62	—	1.0843	31.20	—	
0.2514	1.0942	62.88	9.015	1.0910	49.28	11.000	1.0877	39.15	—	1.0843	31.49	—	
0.3001	1.0946	62.26	9.675	1.0914	48.89	11.775	1.0880	38.91	—	1.0846	31.43	—	
0.3199	1.0947	62.81	9.855	1.0915	49.35	11.960	1.0881	39.29	—	1.0847	31.67	—	
0.3413	1.0954	63.32	9.970	1.0921	49.79	12.110	1.0888	39.67	—	1.0854	32.00	—	

Ionic conductivity

The ionic conductivity of ionic liquids and their IS mixtures are mainly governed by their viscosity and molar concentration. The evolution of the conductivity versus $[\text{NH}_4]\text{[SCN]}$ concentration is plotted in Figure S6, and the data obtained appear in Table S2. The addition of ammonium thiocyanate caused a decrease in conductivity from the pure ionic liquid $[\text{C}_2\text{MIM}][\text{C}_2\text{SO}_4]$ to $x [\text{NH}_4]\text{[SCN]} \approx 0.35$ due to a decrease in the effective mobility of the ionic carrier as a result of the increase in viscosity. From this point up to the solubility limit, conductivity increases because viscosity decreases. This leads to a minimum in conductivity corresponding to a proportion of 1 mole inorganic salt : 2 mole ionic liquid.

In the case of the binary mixture $[\text{C}_2\text{MIM}][\text{OAc}] + [\text{NH}_4]\text{[SCN]}$, the data show that the ionic conductivities increases with the inorganic salt concentration. The results reveal a non-ideal behaviour of these binary mixtures $[\text{C}_2\text{MIM}][\text{OAc}] + [\text{NH}_4]\text{[SCN]}$, because in this composition range the viscosity also increase. This increment is higher when the viscosity stabilizes (from $x [\text{NH}_4]\text{[SCN]} \approx 0.2$ to the solubility limit). As depicted in Figure S6b, an increment of 22 % on the ionic

conductivity from pure ionic liquid $[C_2MIM][OAc]$ to the binary mixture $[C_2MIM][OAc] + [NH_4][SCN]$ with $x [NH_4][SCN] = 0.3413$ is verified.

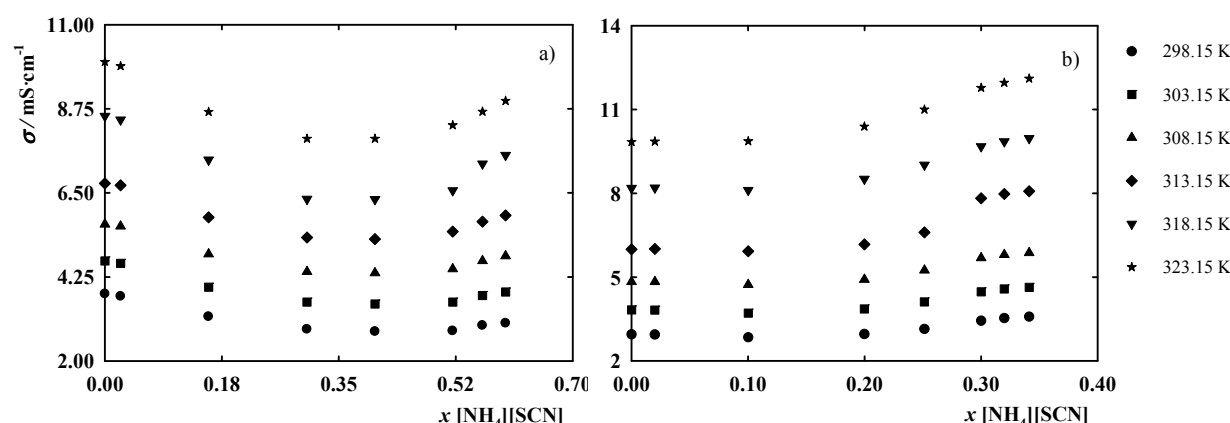


Figure S6. Ionic conductivity as a function of $[NH_4][SCN]$ concentration in the solubility range for the binary systems: (a) $[C_2MIM][C_2SO_4] + [NH_4][SCN]$ and (b) $[C_2MIM][OAc] + [NH_4][SCN]$.

Walden Plot

Different techniques have been used to provide information about the ionicity of pure ionic liquids. The Walden plot is a convenient and versatile tool for measuring the ionicity of these liquids, since it establishes a relationship between the molar conductivity and the viscosity of a solution. In this work, we have used the Walden plot to quantify the investigation of whether the addition of $[NH_4][SCN]$ increases the ionicity of the pure ionic liquids.

Figure S7a is a plot based on the classical concept of the Walden plot for organizing the different possible relations between molar conductivity and fluidity. The straight line fixes the position of the “ideal” Walden line corresponding to an aqueous KCl solution in which the system is known to be fully dissociated and to have ions of equal mobility. For the unit chosen, the ideal line runs from corner to corner of a square diagram.^{S14} The data obtained for the binary system $[C_2MIM][C_2SO_4] + [NH_4][SCN]$ are represented in this plot together with the classification proposed by Angell and co-workers^{S14,S15} for “good” and “poor” ionic liquids. The values obtained for this binary system are similar to those for other pure ionic liquids.^{S16} For each concentration, the Walden plot demonstrates linear behaviour with temperature. If the temperature is fixed (see insert in Figure 7b), increasing the concentration of inorganic salt leads to a binary mixture closer to ideal electrolyte (straight line) whilst, at the three last concentrations, the behaviour reverses.

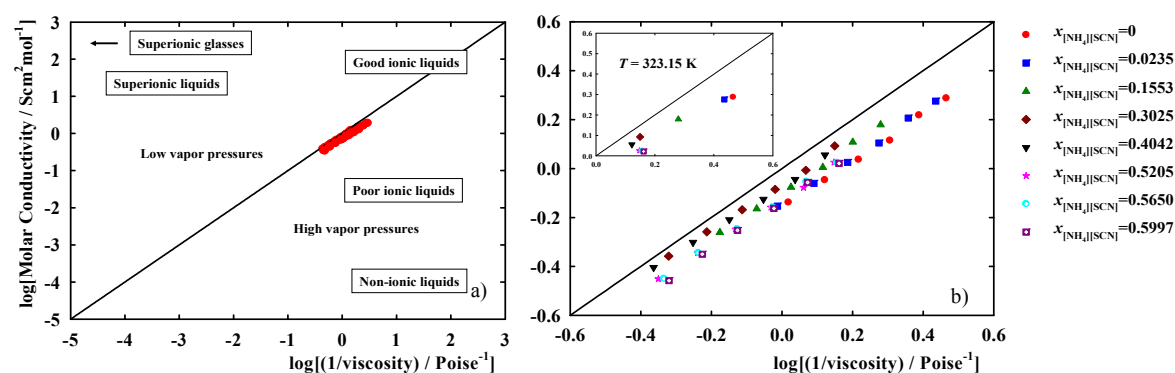


Figure S7. a) Classification diagram for ionic liquids, based on the classical Walden rule, and a Walden plot for the binary system $[C_2MIM][C_2SO_4] + [NH_4][SCN]$. (b) Closer look at the Walden plot for the binary system $[C_2MIM][C_2SO_4] + [NH_4][SCN]$ as a function of inorganic salt concentration. The inside figure shows the behaviour of the binary system at 323.15K.

NMR Studies

NMR studies were used to shed light on the underlying mechanism of solubilisation and to establish the preferential interactions simultaneously with functional groups of both the cations and the anions. The detection and analysis of the chemical shift perturbation ($\Delta\delta$) in NMR spectra have been extensively applied to prove the existence of solvent–solute interactions.^{S17-S21}

Figure S8 shows the ^1H NMR spectrum of the pure $[C_2MIM][C_2SO_4]$. The ^1H and ^{13}C NMR chemical shifts data of neat ionic liquids and the effect of ammonium thiocyanate concentration upon the chemical shifts are depicted in Table S3. A

similar analysis was carried out for the neat inorganic salt $[\text{NH}_4][\text{SCN}]$, as well as the effect of ionic liquid concentration upon the ^1H and ^{13}C NMR chemical shifts of the inorganic salt. These experimental chemical shifts data are shown in Table S4.

The effect of $[\text{NH}_4][\text{SCN}]$ concentration on the ^{13}C NMR spectrum of $[\text{C}_2\text{MIM}][\text{C}_2\text{SO}_4]$ is summarized in Figure S9, where the anion carbons (C9 and C10, in the schematic structure of Figure S8), are highlighted. The signal of the carbon in the CH_2 attached to the sulfate group (C9) moves downfield significantly, indicating that the oxygen atoms of the ethylsulfate anion create stronger interactions with the added inorganic salt than those previously observed in the neat IL between the cation and anion. This downfield change is mostly attributed to the decrease of electron density around the C9 nuclei because the stronger interaction between the oxygen atoms of the sulfate group and the added inorganic salt causes electronic redistribution of the ethylsulfate anion.

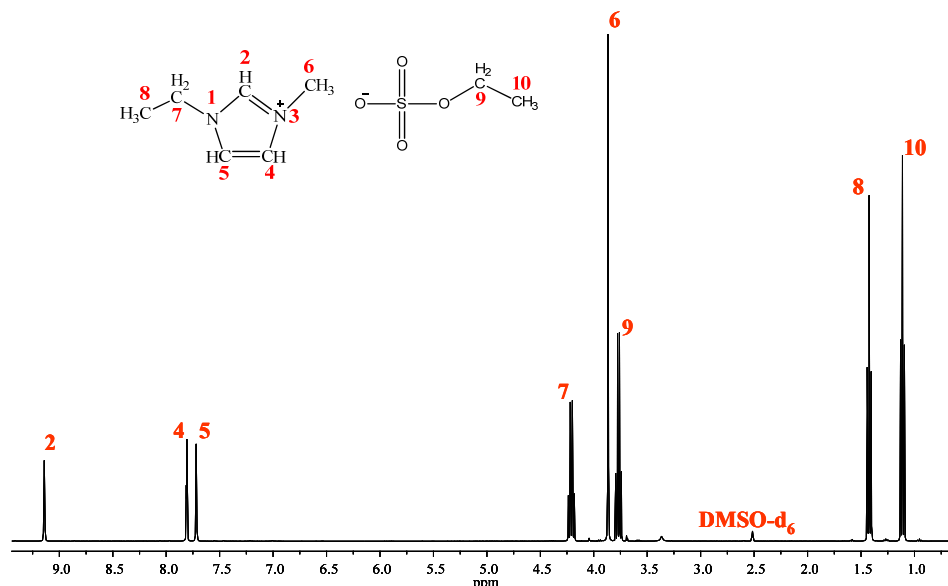


Figure S8. ^1H NMR spectrum of $[\text{C}_2\text{MIM}][\text{C}_2\text{SO}_4]$ in $\text{DMSO}-\text{d}_6$ at 298.15 K. The structure and numbering of the ionic liquid is also depicted.

Table S3. ^1H NMR and ^{13}C NMR chemical shifts (ppm) of $[\text{C}_2\text{MIM}][\text{C}_2\text{SO}_4]$ or $[\text{C}_2\text{MIM}][\text{OAc}]$ and the effect of $[\text{NH}_4][\text{SCN}]$ concentration upon the chemical shifts in $\text{DMSO}-\text{d}_6$ at 298.15 K.

[C ₂ MIM][C ₂ SO ₄]							[C ₂ MIM][OAc]					
Position	Molar fraction of [NH ₄][SCN]						Molar fraction of [NH ₄][SCN]					
	0.000	0.1399	0.2558	0.2979	0.3567	0.4375	0.5708	0.0000	0.1078	0.2047	0.2896	0.3644
^1H NMR												
2	9.136	9.134	9.129	9.128	9.118	9.117	9.110	10.204	10.029	9.773	9.541	9.378
4	7.803	7.801	7.798	7.796	7.789	7.786	7.779	7.935	7.911	7.872	7.845	7.824
5	7.716	7.714	7.710	7.709	7.700	7.698	7.693	7.836	7.815	7.780	7.756	7.736
6	3.863	3.863	3.862	3.862	3.861	3.859	3.856	3.890	3.887	3.881	3.877	3.873
7	4.207	4.207	4.206	4.205	4.203	4.202	4.199	4.233	4.230	4.225	4.220	4.216
8	1.424	1.423	1.422	1.422	1.415	1.416	1.415	1.405	1.407	1.413	1.416	1.418
9	3.763	3.767	3.769	3.768	3.777	3.775	3.775	—	—	—	—	—
10	1.113	1.114	1.115	1.116	1.111	1.113	1.115	1.592	1.633	1.669	1.689	1.696
^{13}C NMR												
2	136.261	136.257	136.247	136.242	136.243	136.228	136.208	137.659	137.415	137.056	136.749	136.513
4	123.529	123.521	123.518	123.519	123.481	123.491	123.492	123.450	123.459	123.474	123.491	123.501
5	121.939	121.933	121.929	121.929	121.899	121.906	121.904	121.923	121.916	121.907	121.910	121.911
6	35.628	35.628	35.634	35.639	35.619	35.636	35.653	35.360	35.407	35.487	35.544	35.594
7	44.074	44.081	44.088	44.092	44.105	44.110	44.122	43.822	43.876	43.954	44.016	44.070
8	15.069	15.062	15.059	15.060	15.028	15.038	15.041	15.167	15.143	15.117	15.094	15.077
9	61.185	61.251	61.294	61.301	61.510	61.477	61.516	173.088	173.292	173.460	173.683	174.051
10	15.069	15.062	15.059	15.060	15.028	15.038	15.041	26.035	25.388	24.752	24.363	24.203

Table S4. ^1H NMR and ^{13}C NMR chemical shifts (ppm) of $[\text{NH}_4]\text{[SCN]}$ and the effect of $[\text{C}_2\text{MIM}]\text{[C}_2\text{SO}_4]$ or $[\text{C}_2\text{MIM}]\text{[OAc]}$ concentration upon the chemical shifts in DMSO-d_6 at 298.15 K.

Position	Molar fraction of $[\text{C}_2\text{MIM}]\text{[C}_2\text{SO}_4]$							Molar fraction of $[\text{C}_2\text{MIM}]\text{[OAc]}$					
	0.000	0.008 ϵ	0.0243	0.0522	0.0775	0.1175	0.2505	0.0000	0.0079	0.0687	0.1106	0.2006	0.2886
^1H NMR													
11	7.056	7.071	7.077	7.065	7.075	7.069	7.081	7.056	7.048	6.980	6.935	6.969	6.993
^{13}C NMR													
12	130.609	130.36	130.256	130.481	130.359	130.510	130.431	130.609	130.382	130.106	130.114	130.253	130.383

Figure S10 and S11 show the ^1H and ^{13}C NMR spectra of the pure $[\text{C}_2\text{MIM}]\text{[OAc]}$ and $[\text{NH}_4]\text{[SCN]}$, respectively. The relative changes of proton chemical shifts in $[\text{C}_2\text{MIM}]\text{[OAc]}$ ^1H and ^{13}C NMR spectra with increasing inorganic salt concentration are depicted in Figure S12. As illustrated in Figure S12a, the ring protons of the imidazolium cation (H_2 , H_4 and H_5 ; numbers in the schematic structures in Figure S10) shown a upfield shift, while a negligible change is observed in the other protons of the cation and anion with increasing inorganic salt concentration. The most acidic H_2 proton in the imidazolium cation presents the greatest upfield shift as compared to the H_4 and H_5 protons. The effect of $[\text{NH}_4]\text{[SCN]}$ concentration on the ^1H NMR spectra of the $[\text{C}_2\text{MIM}]\text{[OAc]}$ IL are depicted in Figure S13, where the upfield shift trend of the ring protons of the imidazolium cation with increasing inorganic salt concentration is highlighted. Figure S12b illustrates the trend of the chemical shift differences of carbons in ^{13}C NMR of $[\text{C}_2\text{MIM}]\text{[OAc]}$ with increasing concentration of inorganic salt. The effect of $[\text{NH}_4]\text{[SCN]}$ concentration on the ^{13}C NMR spectra of $[\text{C}_2\text{MIM}]\text{[OAc]}$ is summarized in Figure S14-S15, where the distinct behaviour of the anion carbons are highlighted. The signal of the carbon in the carboxyl group (C_9) moves downfield significantly, while the carbon of methyl group (C_{10}) present upfield change. The significant downfield variation on the carboxyl signal indicates that the acetate anions create stronger interactions with the added inorganic salt^{S22} than those previously observed in the neat pure ionic liquid between the cation and anion. The upfield variation of the carbon of methyl group is mostly attributed to the increase of electron density around the C_{10} nuclei, as result of the electronic redistribution on the acetate anion due to the stronger interaction between the carboxyl group and the added ammonium thiocyanate.

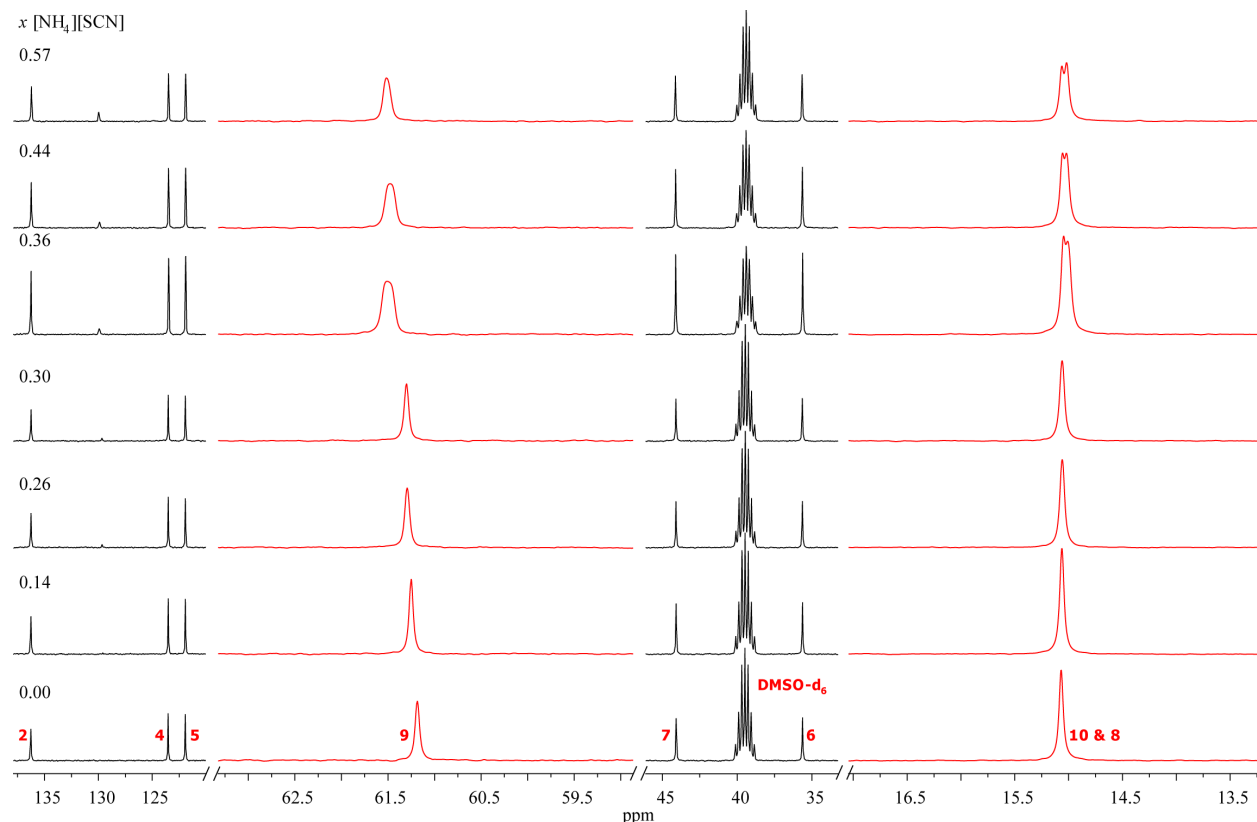


Figure S9. Effect of $[\text{NH}_4]\text{[SCN]}$ concentration on the ^{13}C NMR spectrum of $[\text{C}_2\text{MIM}]\text{[C}_2\text{SO}_4]$ in DMSO-d_6 . The anion carbons are highlighted in red, and the bottom spectrum is the neat $[\text{C}_2\text{MIM}]\text{[C}_2\text{SO}_4]$.

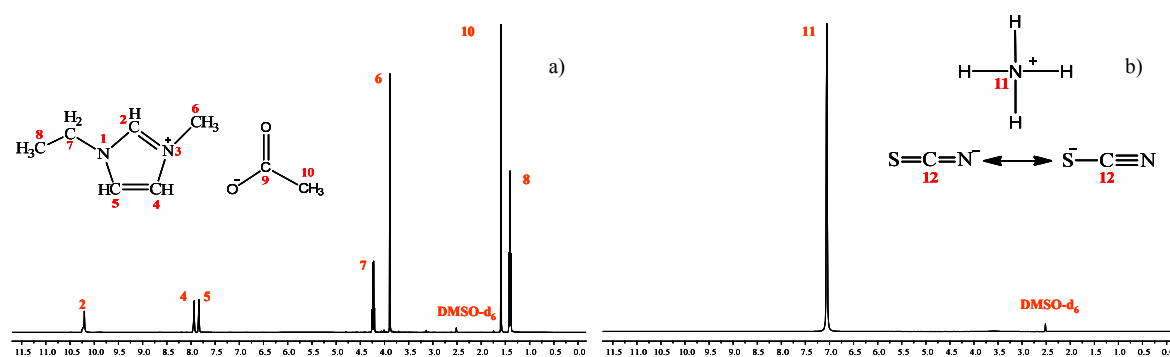


Figure S10. ^1H NMR spectra of: (a) $[\text{C}_2\text{MIM}][\text{OAc}]$ and (b) $[\text{NH}_4][\text{SCN}]$ in $\text{DMSO}-\text{d}_6$ at 298.15 K. The structure and numbering of ionic liquid and inorganic salt are also depicted.

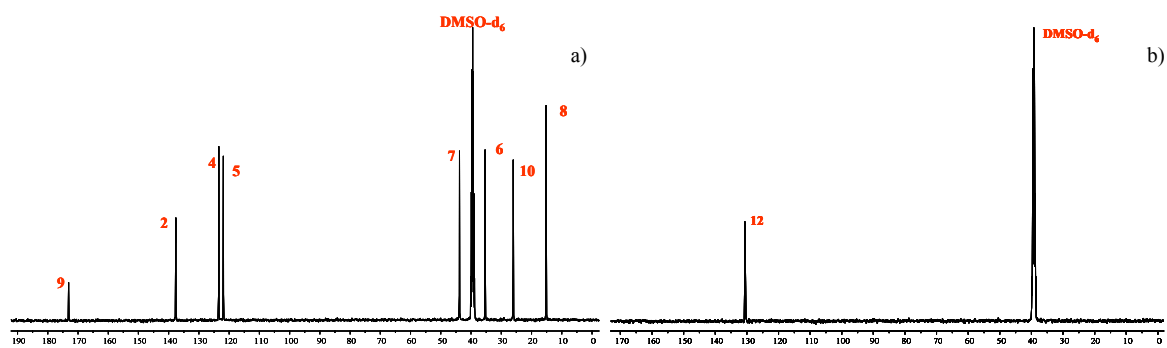


Figure S11. ^{13}C NMR spectra of: (a) $[\text{C}_2\text{MIM}][\text{OAc}]$ and (b) $[\text{NH}_4][\text{SCN}]$ in $\text{DMSO}-\text{d}_6$ at 298.15 K.

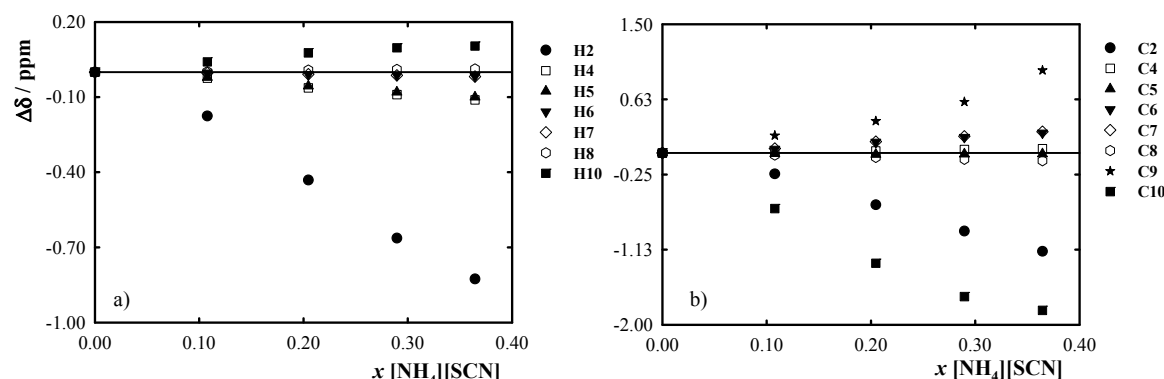


Figure S12. Trend of the chemical shift difference of: (a) protons in ^1H NMR of $[\text{C}_2\text{MIM}][\text{OAc}]$; and (b) carbons in ^{13}C NMR of $[\text{C}_2\text{MIM}][\text{OAc}]$ with increasing $[\text{NH}_4][\text{SCN}]$ concentration ($\Delta\delta = \delta - \delta_{\text{neat}}$). The line represents the $\Delta\delta = 0$ (chemical shift of the pure ionic liquid).

The relative changes of proton and carbon chemical shifts in the $[\text{NH}_4][\text{SCN}]$ ^1H and ^{13}C NMR spectra with increasing $[\text{C}_2\text{MIM}][\text{OAc}]$ molar concentration are illustrated in Figure S14. Both proton, H11, and carbon, C12, show upfield changes but present a minimum at $x [\text{C}_2\text{MIM}][\text{OAc}] \approx 0.05$. This molar composition is a threshold point: from this composition onwards the interactions between IS and IL begin to be more stable than those found for values ≤ 0.05 .^{S18} This relative stability then increases with IL molar concentration and proves the complex nature of the interactions between the IL and the IS, both at the IL-rich and IS-rich sides (Figures S12–S15).

The NMR studies clearly demonstrate the occurrence of interactions between the ionic liquid and the inorganic salt, and that these interactions alter the structures of the neat ionic liquid, as well as of the pure $[\text{NH}_4][\text{SCN}]$ inorganic salt, and that the interactions behaviour is dependent of the inorganic salt concentration. From the NMR results, as well as from the Walden plot analysis (increase of the IL ionicity), it is obvious that a new class of ionic liquids, the High Ionicity Ionic Liquids (HIILs) arise from the fine-tuned addition of a inorganic salt to a ionic liquid.

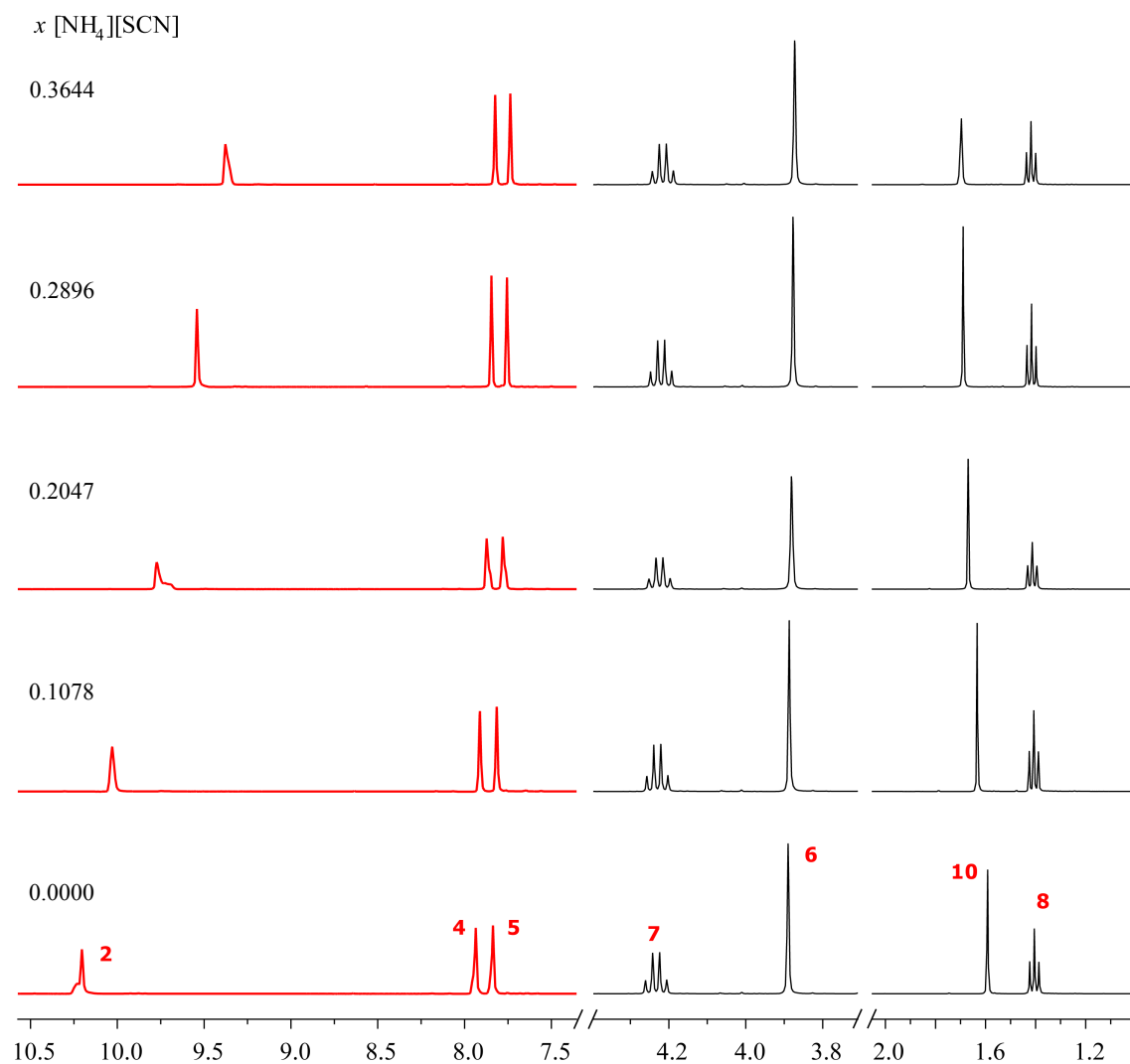


Figure S13. Effect of $[\text{NH}_4]\text{[SCN]}$ concentration on the ^1H NMR spectrum of $[\text{C}_2\text{MIM}]\text{[OAc]}$ in DMSO-d_6 . The ring protons (H_2 , H_4 , and H_5) of the imidazolium cation are highlighted, showing an upfield shift, especially the most acidic H_2 proton. The bottom spectrum is the neat $[\text{C}_2\text{MIM}]\text{[OAc]}$.

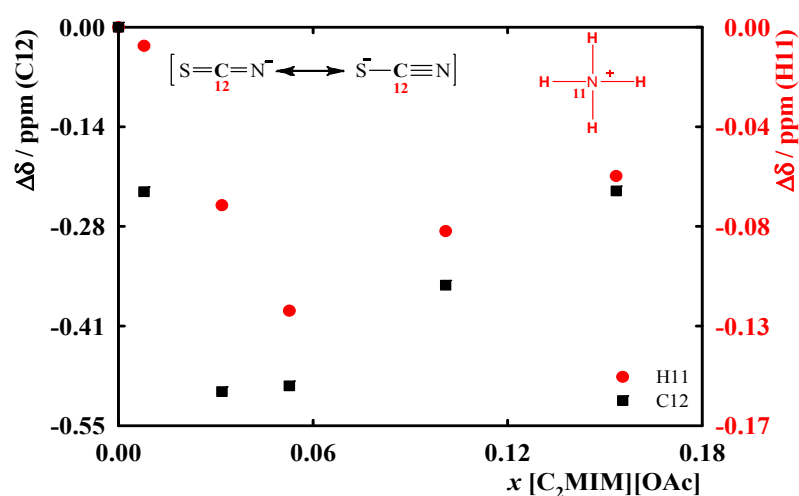


Figure S14. Trend in the chemical shift difference of protons in ^1H NMR and carbons in ^{13}C NMR of $[\text{NH}_4]\text{[SCN]}$ with increasing $[\text{C}_2\text{MIM}]\text{[OAc]}$ molar concentration ($\Delta\delta = \delta - \delta_{\text{neat}}$).

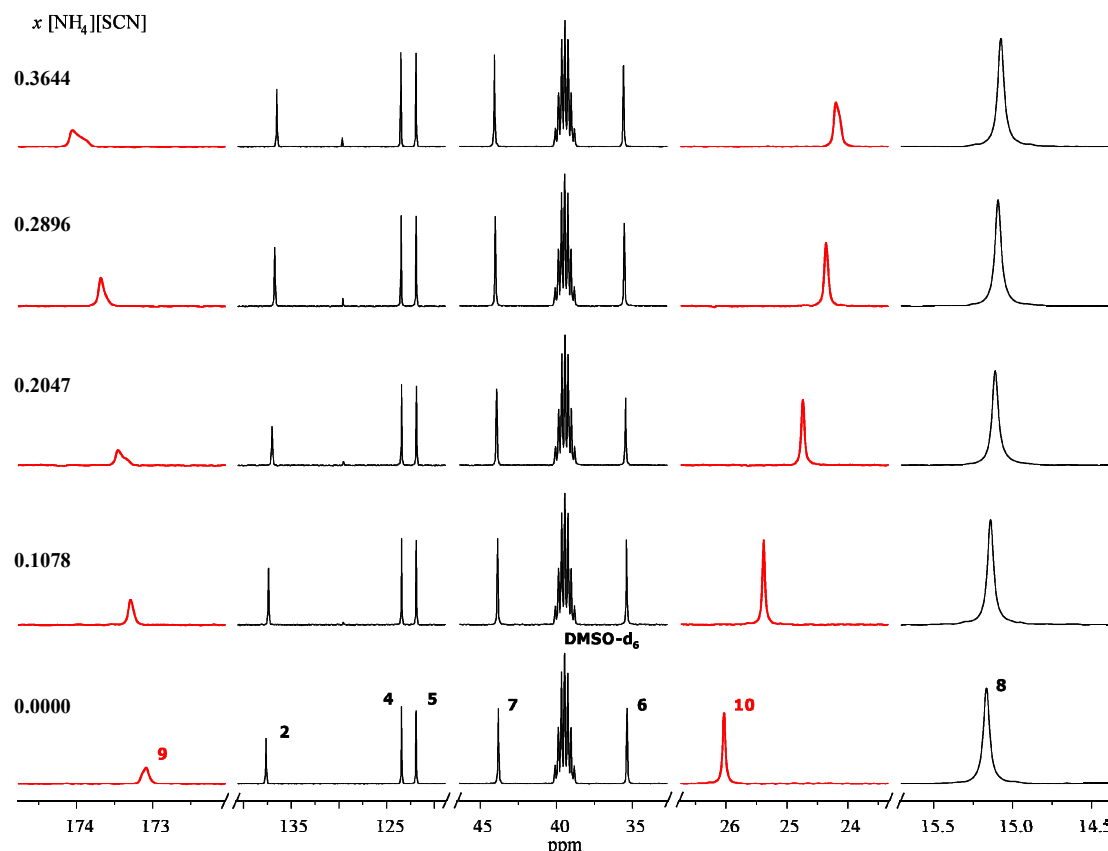


Figure S15. Effect of $[\text{NH}_4]\text{[SCN]}$ concentration on the ^{13}C NMR spectrum of $[\text{C}_2\text{MIM}]\text{[OAc]}$ in DMSO-d_6 . The anion carbons are highlighted, disclosing distinct behaviours. A significant downfield variation on the carboxyl (C9) signal is verified, as well as an upfield shift of the methyl carbon (C10). The bottom spectrum is the neat $[\text{C}_2\text{MIM}]\text{[OAc]}$.

Computational Methods

Molecular Dynamics (MD) Simulations

Molecular modeling and simulation include computational techniques developed within the frameworks of quantum or statistical mechanics that are able to analyze the links between the macroscopic behavior of matter and its characteristics at a molecular level. Modeling and simulation studies are traditionally used either as predictive or interpretative research instruments but in the case of ionic liquids—a relatively recent research front—they have also assumed the role of exploratory tools leading to some important discoveries that were only later corroborated by experimental data. For example, one of the first works dealing with the recognition of neat ionic liquids as nano-segregated media originated from molecular dynamics (MD) studies.^{S23} The MD study of the solvation process of different solutes in IL media has been analyzed in subsequent publications.^{S24} In other words, the knowledge about the physical chemistry of ionic liquids is rapidly advancing through the interplay between experiments, theory and modeling, each providing challenges, guidelines and checks to the others.

The molecular dynamics runs on the different ionic liquids solutions were performed using the DL_POLY package version 2.20.^{S25} The simulation boxes were prepared by random distribution of the ionic liquid and salt ions to give $[\text{NH}_4]\text{[SCN]}$ mole fractions of 0, 0.1, 0.33 for $[\text{C}_2\text{MIM}]\text{[OAc]}$ and 0, 0.1, 0.33 and 0.5 for $[\text{C}_2\text{MIM}]\text{[C}_2\text{SO}_4]$. A cutoff distance of 14 Å was used in all simulations and the Ewald summation technique (k -values set to 5 and $\alpha = 0.185$ Å) was applied to account for long-range Coulomb interactions beyond those cutoff distances. The simulations were performed at 298 K and 0.1 MPa, under isothermal-isobaric ($N-p-T$) ensemble. Typical runs consisted of an equilibration period of ≈ 1 ns followed by a production of 8 ns.

The force field developed by Canongia Lopes and coworkers^{S26–S27} was selected to describe the inter- and intra-molecular interactions of the ionic liquid. Since, to the best of our knowledge, no force field for $[\text{NH}_4]\text{[SCN]}$ in non aqueous solutions has been reported, a new parameterization compatible with the OPLS-AA force-field was used, assuming that these small ions behave as rigid entities. The geometric parameters were calculated at the MP2/aug-cc-pVQZ^{S28–S33} theoretical level using Gaussian-03 package,^{S36} and the atomic point charges for the different atoms were obtained with the CHelpG methodology,^{S37} has implemented in Gaussian-03, at the same theoretical level. The nonbonded (Lennard-Jones) parameters were retrieved from literature data and are shown in Table S5 together with the computed geometric parameters for $[\text{NH}_4]\text{[SCN]}$.

Table S5. Bonded and nonbonded parameters for $[\text{NH}_4]^+[\text{SCN}]^-$ used in the molecular dynamics simulations.

Nonbonded				
	Atoms	q / e	$\sigma / \text{\AA}$	$\epsilon / \text{kJ}\cdot\text{mol}^{-1}$
$[\text{NH}_4]^+$	NT	-0.748	3.25 ^a	0.7113 ^a
	HT	0.437	2.50 ^b	0.1255 ^b
$[\text{SCN}]^-$	Sy	-0.737	3.52 ^c	1.5225 ^c
	Cy	0.517	3.35 ^c	0.4250 ^c
	Ny	-0.780	3.31 ^c	0.3100 ^c
Bonded				
Bonds	$r / \text{\AA}$	Angles		θ / deg
NT–HT	1.027	HT–NT–HT		109.47
Sy–Cy	1.679	Sy–Cy–Ny		180.00
Cy–Ny	1.207			

^a reference S38; ^b reference S27; ^c reference S39.

Funding Sources

Fundaçao para a Ciéncia e Tecnologia through Projects: PTDC / QUI / 72903 / 2006, PTDC / QUI / 71331 / 2006, PTDC/EQU-EPR/104554/2008 and PTDC / EQU – FTT / 116015 / 2009. The NMR spectrometers are part of the National NMR Network and were purchased within the framework of the National Program for the Renovation of Scientific Equipment, contract REDE / 1517 / RMN / 2005, with funds from POCI 2010 (FEDER) and FCT / MCTES.

ACKNOWLEDGMENT

A. B. Pereiro acknowledges Marie Curie Actions – Intra–European Fellowships (IEF) for a contract under FP7–PEOPLE–2009–IEF – 252355 – HALOGENILS. J. M. M. Araújo and F. S. Oliveira gratefully acknowledge the financial support of FCT/MCTES (Portugal) through the Post-Doc grant SFRH/BPD/65981/2009 and through the PhD fellowship SFRH/BD/73761/2010. J. M. S. S. Esperança and I. M. Marrucho acknowledge FCT/MCTES (Portugal) for a contract under Programa Ciéncia 2007.

REFERENCES

- (S1) F. J. Deive, A. Rodriguez, A. B. Pereiro, K. Shimizu, P. A. S. Forte, C. C. Romao, J. N. C. Lopes, J. M. S. S. Esperanca and L. P. N. Rebelo, *J. Phys. Chem. B*, 2010, **114**, 7329.
(S2) A. J. L. Costa, M. R. C. Soromenho, K. Shimizu, I. M. Marrucho, J. M. S. S. Esperanca, J. N. C. Lopes and L. P. N. Rebelo, *Chem. Phys. Chem.*, 2011, submitted for publication.
(S3) M. Tariq, P. J. Carvalho, J. A. P. Coutinho, I. M. Marrucho, J. N. C. Lopes and L. P. N. Rebelo, *Fluid Phase Equilib.*, 2011, **301**, 22.
(S4) X. Paredes, O. Fandíño, M. J. P. Comuñas, A. S. Pensado and J. Fernández, *J. Chem. Thermodyn.*, 2009, **41**, 1007.
(S5) O. Klug and B. A. Lopatin, *New developments in conductimetric and oscillosmetric analysis*, Elsevier Science Publisher, Amsterdam, 1988.
(S6) J. Hamelin, T. K. Bose and J. Thoen, *Phys. Rev. A*, 1990, **42**, 4735.
(S7) F. J. V. Santos, C. A. N. de Castro, P. J. F. Mota and A. P. C. Ribeiro, *Int. J. Thermophys.*, 2010, **31**, 1869.
(S8) J. A. Widegren, E. M. Saurer, K. N. Marsh and J. W. Magee, *J. Chem. Thermodyn.*, 2005, **37**, 569.
(S9) J. A. Widegren and J. W. Magee, *J. Chem. Eng. Data*, 2007, **52**, 2331.
(S10) J. S. Moulthrop, R. P. Swatloski, G. Moyna and R. D. Rogers, *Chem. Commun.*, 2005, 1557; D. A. Fort, R. P. Swatloski, P. Moyna, R. D. Rogers and G. Moyna, *Chem. Commun.*, 2006, 714.
(S11) N. Srivastava and S. Chandra, *Phys. Stat. Sol. (a) – Applied Research*, 1997, **163**, 313.
(S12) C. Guha, J. M. Chakraborty, S. Karanjai and B. Das, *J. Phys. Chem. B*, 2003, **107**, 12814.
(S13) M. Gadermann, D. Vollmar and R. Signorell, *Phys. Chem. Chem. Phys.*, 2007, **9**, 4535.
(S14) W. Xu, E. I. Cooper and C. A. Angell, *J. Phys. Chem. B*, 2003, **107**, 6170.
(S15) C. A. Angell, N. Byrne and J.-P. Belieres, *Accounts Chem. Res.*, 2007, **40**, 1228.
(S16) D. R. MacFarlane, M. Forsyth, E. I. Izgorodina, A. P. Abbott, G. Annat and K. Fraser, *Phys. Chem. Chem. Phys.*, 2009, **11**, 4962.
(S17) A. G. Avent, P. A. Chaloner, M. P. Day, K. R. Seddon and T. Welton, *J. Chem. Soc.-Dalton Trans.*, 1994, **23**, 3405.
(S18) J. M. M. Araújo, R. Ferreira, I. M. Marrucho and L. P. N. Rebelo, *J. Phys. Chem. B*, 2011, **115**, 10739.
(S19) M. R. Chierotti and R. Gobetto, *Chem. Commun.*, 2008, 1621.
(S20) E. Yashima, C. Yamamoto and Y. Okamoto, *J. Am. Chem. Soc.*, 1996, **118**, 4036.
(S21) C. L. McCormick, P. A. Callais and B. H. Hutchinson, *Macromolecules*, 1985, **18**, 2394.
(S22) R. Hagen and J. D. Roberts, *J. Am. Chem. Soc.*, 1969, **91**, 4504.
(S23) J. N. C. Lopes and A. A. H. Padua, *J. Phys. Chem. B*, 2006, **110**, 3330.
(S24) J. N. C. Lopes, M. F. C. Gomes and A. A. H. Padua, *J. Phys. Chem. B*, 2006, **110**, 16816; A. A. H. Padua, M. F. C. Gomes and J. N. C. Lopes, *Accounts Chem. Res.*, 2007, **40**, 1087.
(S25) W. Smith and T. R. Forester, *The DL_POLY Package of Molecular Simulation Routines (v.2.20)*, The Council for The Central Laboratory of Research Councils, Daresbury Laboratory: Warrington, 2006.
(S26) J. N. Canongia Lopes, J. Deschamps and A. A. H. Pádua, *J. Phys. Chem. B*, 2004, **108**, 2038.

- (S27) J. N. Canongia Lopes, A. A. H. Padua and K. Shimizu, *J. Phys. Chem. B*, 2008, **112**, 5039.
(S28) M. Headgordon, J. A. Pople and M. J. Frisch, *Chem. Phys. Lett.*, 1988, **153**, 503.
(S29) S. Saebo and J. Almlöf, *Chem. Phys. Lett.*, 1989, **154**, 83.
(S30) M. J. Frisch, M. Headgordon and J. A. Pople, *Chem. Phys. Lett.*, 1990, **166**, 275.
(S31) M. J. Frisch, M. Headgordon and J. A. Pople, *Chem. Phys. Lett.*, 1990, **166**, 281.
(S32) M. Headgordon and T. Headgordon, *Chem. Phys. Lett.*, 1994, **220**, 122.
(S33) T. H. Dunning, *J. Chem. Phys.*, 1989, **90**, 1007.
(S34) G. de Oliveira, J. M. L. Martin, F. de Proft and P. Geerlings, *Phys. Rev. A*, 1999, **60**, 1034.
(S35) R. A. Kendall, T. H. Dunning and R. J. Harrison, *J. Chem. Phys.*, 1992, **96**, 6796.
(S36) M. J. Frisch, G. W. Trucks, H. B. Schlegel, G. E. Scuseria, M. A. Robb, J. R. Cheeseman, J. J. A. Montgomery, T. Vreven, K. N. Kudin, J. C. Burant, J. M. Millam, S. S. Iyengar, J. Tomasi, V. Barone, B. Mennucci, M. Cossi, G. Scalmani, N. Rega, G. A. Petersson, H. Nakatsuji, M. Hada, M. Ehara, K. Toyota, R. Fukuda, J. Hasegawa, M. Ishida, T. Nakajima, Y. Honda, O. Kitao, H. Nakai, M. Klene, X. Li, J. E. Knox, H. P. Hratchian, J. B. Cross, V. Bakken, C. Adamo, J. Jaramillo, R. Gomperts, R. E. Stratmann, O. Yazyev, A. J. Austin, R. Cammi, C. Pomelli, J. W. Ochterski, P. Y. Ayala, K. Morokuma, G. A. Voth, P. Salvador, J. J. Dannenberg, V. G. Zakrzewski, S. Dapprich, A. D. Daniels, M. C. Strain, O. Farkas, D. K. Malick, A. D. Rabuck, K. Raghavachari, J. B. Foresman, J. V. Ortiz, Q. Cui, A. G. Baboul, S. Clifford, J. Cioslowski, B. B. Stefanov, G. Liu, A. Liashenko, P. Piskorz, I. Komaromi, R. L. Martin, D. J. Fox, T. Keith, M. A. Al-Laham, C. Y. Peng, A. Nanayakkara, M. Challacombe, P. M. W. Gill, B. Johnson, W. Chen, M. W. Wong, C. Gonzalez and J. A. Pople, *Gaussian 03, Revision C.02*, Gaussian, Inc.: Wallingford, 2004.
(S37) C. M. Breneman and K. B. Wiberg, *J. Comput. Chem.*, 1990, **11**, 361.
(S38) W. L. Jorgensen and J. Gao, *J. Phys. Chem.*, 1986, **90**, 2174.
(S39) A. Botti, S. E. Pagnotta, F. Bruni and M. A. Ricci, *J. Phys. Chem. B*, 2009, **113**, 10014.